IEEE Photonics Journal
An IEEE Photonics Society Publication

Open Access

Experimental Study and Application of Response Mask Invariant Characteristic for Generalized Visible Light Communication Channel

Volume 10, Number 3, June 2018

Fangzhou Wu
Li Chen
Shaoyang Cai
Weidong Wang

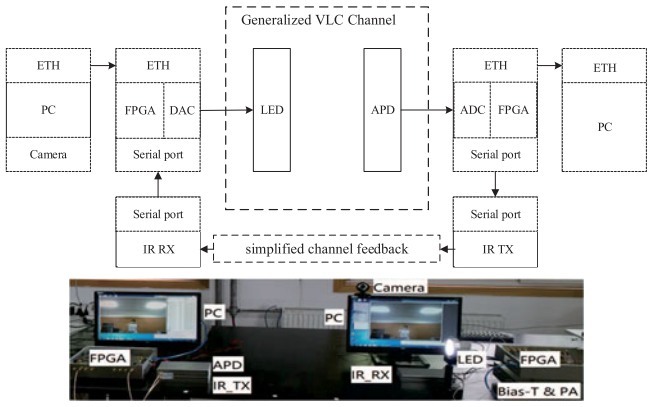

DOI: 10.1109/JPHOT.2018.2834384
1943-0655 © 2018 IEEE

IEEE photonics SOCIETY

IEEE

Experimental Study and Application of Response Mask Invariant Characteristic for Generalized Visible Light Communication Channel

Fangzhou Wu, Li Chen, Shaoyang Cai, and Weidong Wang

Optical-Wireless Communication Key Lab of Chinese Academy of Sciences, University of Science and Technology of China, Hefei 230027, China

DOI:10.1109/JPHOT.2018.2834384

Manuscript received April 10, 2018; accepted May 4, 2018. Date of publication May 8, 2018; date of current version May 29, 2018. This work was supported in part by the National Science and Technology Major Project of China MIIT under Grant 2017ZX03001003-003, in part by the National Natural Science Foundation of China under Grant 61601432, and in part by the Fundamental Research Funds for the Central Universities. Corresponding author: L. Chen (e-mail: chenli87@ustc.edu.cn).

Abstract: In this paper, we describe a generalized visible light communication (VLC) channel, which consists of the frequency responses of the light emitting diode (LED), the wireless optical channel, and the photo detector (PD). Based on the theoretical analysis of the generalized VLC channel, we found the response mask invariant characteristic (RMIC) under the condition of strong line of sight components, which means the shape of frequency response of generalized VLC channel is time-independent and invariant at different distances of the transceivers, different emitting angles of the LED and different incident angles of the PD. Depending on the RMIC, the shapes of received spectrum and signal-to-noise rate are also invariant. The experimental platform was set up to verify the proposed RMIC. Furthermore, a predefined VLC system with a new channel feedback method is described, both the complexity and time cost of feedback can greatly reduce through the proposed channel feedback method.

Index Terms: VLC, generalized VLC channel, response mask invariant characteristic, channel feedback

1. Introduction

Visible Light Communication (VLC) utilizing Light Emitting Diode (LED) can provide communication service while lighting. Its main features are free of electromagnetic interference and large license-free bandwidth which is 10,000 times as wide as the radio's [1]. In addition, visible light cannot pass through walls, which provides a secure communication condition. For these reasons, VLC has become a strong complement to Radio Frequency (RF) communications.

A typical VLC system usually consists of LED, wireless optical channel and Photo Detector (PD). Their impacts on the communication performance of VLC system had been individually discussed in [2]–[15]. Lee *et al.* introduced how to model the wireless optical channel through the method of analyzing Infrared (IR) channel, and they simulated the wireless optical channel in a typical indoor environment (cubic room, 5 m $\times$ 5 m $\times$ 3 m) [2]. However, the nonlinearity influences of LEDs and the noise characteristics of PD are not taken into account. [3] modeled

the wireless optical channel based on iterative site-based method in case that optical devices (the LEDs and the PD) are ideal. In [4], the wireless optical channel was modeled by using a ray tracing method, and some simulation results have been presented. Although the method has low computational complexity, only considering the wireless optical channel is not enough to analyze the communication performance of VLC system. For optical wireless communication, the effect of the nonlinearity of LEDs was discussed [5], [6], [7] demonstrated that the nonlinearity of LEDs can be mitigated by equalization techniques while it only considered the distortion caused by the nonlinearity of LEDs. In [8], it noted that we should consider the effects of thermal noise and shot noise in VLC system. In addition to LEDs, electrical devices such as Digital-to-Analog Converters (DACs), Analog-to-Digital Converters (ADCs), amplifiers and Photo-Diodes (PDs) may bring nonlinear distortions in VLC systems [12]. In [13], the author proposed a method to mitigate the nonlinear distortion in amplifier links. Since the PDs work in a narrow range, the distortion is not the key influence compared with LEDs [14]. Besides, The mitigation of ADCs has been studied in [15]. To the best of our knowledge, the existing works including the above mentioned ones only focus on the modeling of wireless optical channel. Nonetheless, in VLC system, the signals experience the electric-optical conversion and optical-electric conversion (E-O-E) from the transmitter to the receiver. To analyze the communication performance in electronic domain for VLC system, it is necessary to consider the LED, the wireless optical channel and the PD at the same time. From the above, we describe the generalized VLC channel, which consists of the frequency responses of the LED, the wireless optical channel and the PD.

In order to achieve a high transmission rate, many novel techniques have been applied to VLC system. In VLC, visible light is non-coherent light, which has broadband spectrum and random phase [2]. Therefore we transmit the information by the intensity of visible light which is called by Intensity Modulation and Direct Detection (IM/DD) [1]. Orthogonal Frequency Division Multiplexing (OFDM), as a widely solution for Inter-Symbol Interference (ISI) caused by the dispersive channel, is used in a range of optical systems. For IM/DD systems, to satisfy the constraints where the base-band signal must be unipolar, various OFDM techniques for IM/DD system has been proposed such as Direct Current biased Optical OFDM (DCO-OFDM) [16], Asymmetrically Clipped Optical OFDM (ACO-OFDM) [17], and Unipolar OFDM (U-OFDM) [18]. Furthermore, adaptive bits allocation techniques are adopted in order to make better use of the frequency resources of VLC system [19], [20]. However, the algorithms mentioned above need channel estimation and feedback for every time slot as in RF communication, which may not be a cost-efficient approaches since the receiver should send complete Channel State Information (CSI) to the transmitter for link adaptation. Fortunately, we describe a novel channel feedback method to solve that problem.

In this paper, based on the theoretical analysis of the generalized VLC channel, we propose the Response Mask Invariant Characteristic (RMIC) under the condition of strong Line Of Sight (LOS) components, which means the shape of frequency response of generalized VLC channel is time-independent and unchanged at different distances of the transceivers, different emitting angles of the LED and different incident angles of the PD. The RMIC improves the way of channel feedback, and both the complexity of channel feedback and the data for channel feedback significantly reduce. In order to illustrate that, we describe a new channel feedback method for the VLC-OFDM system. Our contributions can be summarized as follows:

- *The Proposed RMIC*. We propose the RMIC for the generalized VLC channel. It is the main feature of generalized VLC channel and quite different with the feature of RF channel;
- *Experimental Study for RMIC*. We design the experiments at different distances of the transceivers, different incident angles of the PD and different vertical offsets. We find that the experimental results verify the RMIC;
- *Predefined VLC-OFDM System*. Based on RMIC, we design a predefined VLC-OFDM system with novel simplified channel feedback. Under the predefined VLC-OFDM system, both the complexity of channel feedback and the data for feedback CSI significantly reduce.

The remainder of this paper is organized as follows. In Section II, the theoretical analysis of RMIC is introduced in detail. Experimental study is presented and the results are analyzed in Section III. Under RMIC, we design a predefined VLC-OFDM system with proposed simplified

channel feedback. the performance of new VLC-OFDM system is shown in Section IV. The paper concludes in Section V.

2. Theoretical Analysis

2.1 Channel Model for RMIC

In the theoretical analysis, we only consider the channel model of VLC system based on a single lighting source. The reasons are as follows:

Firstly, under illumination constraints, the practical system usually uses a cluster of LEDs for lighting. For a cluster of LEDs, the distance between the LEDs is much smaller than the distance between PD and the LEDs. Without loss of generality, both of a single LED and a cluster of LEDs can be modeled as a single lighting source.

Secondly, for multiple lighting sources in a room, every lighting source is an Optical Access Point (OAP). With Time-Division Multiple Access (TDMA), non-overlapping time slots are allocated to different users based on the requested data rates and Quality of Service (QoS) [21]. And per user is connected to an OAP in per time slot, which can be modeled as point-to-point communication.

2.2 Response Mask Invariant Characteristic

In this section, we will demonstrate and explain RMIC which means the shape of frequency response of generalized VLC channel is fixed and determined by the type of LED. Besides, according to RMIC, the shape of spectrum of the received signals have the same shape of received SNR.

In [8], [22], the impulse response of generalized VLC channel is given by

$$h(t) = h_{LED}(t) \otimes h_{op}(t) \otimes h_{PD}(t), \tag{1}$$

where $h_{LED}(t)$ is the impulse response of LED, $h_{op}(t)$ represents the impulse response of wireless optical channel, the impulse response of PD is $h_{PD}(t)$, and $\otimes$ denotes convolution.

$h_{LED}(t)$ is determined by the characteristics of LED [22], it means the LEDs with different types have different impulse responses. However, $h_{PD}(t)$ can be regarded as a constant k_{PD} and depends on the type of PD because the response bandwidth of PD is far greater than the modulation bandwidth of LED [22]. Depending on [2], [23], the characteristics of wireless optical channel can be approximately determined by the strong LOS components. Thus, $h_{op}(t)$ can be written as

$$h_{op}(t) = h_{op}^{(0)}(t) = \frac{m+1}{2\pi}\cos^m(\phi)\cos(\theta)\frac{A_{eff}}{d^2} \times \mathrm{rect}\left(\frac{\theta}{FOV}\right)\delta\left(t - \frac{d}{c}\right). \tag{2}$$

where m is the order of Lambertian emission, ϕ, θ, FOV (field of view) are the emitting angle of LED, the incident angle of PD and the PD detection angle, respectively. Apart from this, A_{eff} presents the effective area of the PD, d is the distance between transceivers, c is the speed of light, $\delta(.)$ denotes the Dirac delta function and rect(x) is the rectangular function.

The corresponding frequency domain expression in the discrete form is given by

$$H_{op}(k) = \sum_{n=0}^{N-1} h_{op}(n) e^{-j\frac{2\pi}{N}kn} = k_{op}(\theta, d) e^{-j\frac{2\pi}{N}kt_0}, \tag{3}$$

where $k_{op}(\theta, d) = (m+1)/(2\pi) \cdot \cos^m(\phi)\cos(\theta) \cdot A_{eff}/d^2 \cdot rect(\theta/FOV)$ is time-independent and determined by the position of transceivers. $t_0 = d/c$ is the delay caused by the distance between the transceivers.

Therefore, from (1) and [17], we can obtain the frequency domain signal through generalized VLC channel in the discrete form, which can be given by

$$X_{rx}(k) = X_{dc}(k) H_{LED}(k) H_{op}(k) H_{PD}(k) + W(k), \tag{4}$$

where $H_{LED}(k)$, $H_{op}(k)$, $H_{PD}(k)$ are the frequency response of LED, the frequency response of wireless optical channel and the frequency response of PD, respectively. $X(K) = a(K) + jb(K)$ is a

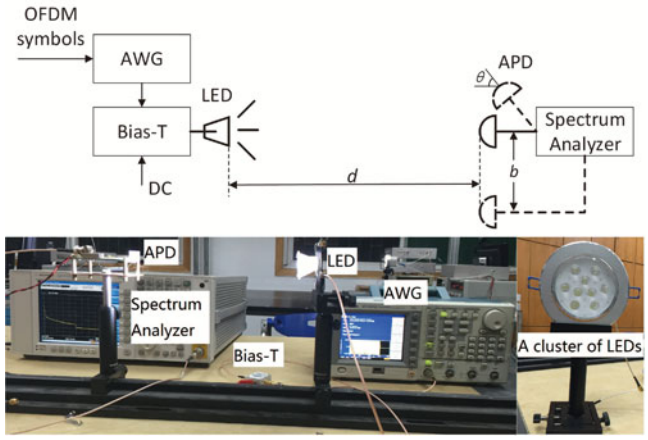

Fig. 1. The structure of experimental VLC system.

zero mean complex random variable with variance σ_K^2 and $W(k)$ is the sum noise (ambient noise, shot noise and thermal noise), which is modeled as Gaussian noise with zero mean and variance N_0 [23].

The received SNR in the kth sub-carrier in the logarithmic form is

$$\begin{aligned}\log(SNR_k) &= \log\left(\frac{|H_{LED}(k)\,H_{op}(k)\,H_{PD}(k)|^2 E[|X_{dc}(k)|^2]}{N_0}\right)\\ &= \underbrace{\log(k_{op}(\theta,d)^2)+\log(k_{PD}^2\left|H_{LED}(k)\right|^2)}_{\triangleq\alpha}+\log(\sigma_k^2/N_0)\end{aligned} \tag{5}$$

where k_{PD} is photoelectric conversion efficiency of PD, which is constant and depends on the type of PD, $k_{op}(\theta, d)$ is related to the position of transceivers, and $\alpha \triangleq \log(k_{op}(\theta,d)^2)+\log(k_{PD}^2\left|H_{LED}(k)\right|^2)$ is the shape of frequency response of generalized VLC channel.

Following Eq. (5), α shows that the shape of frequency response of generalized VLC channel is time-independent and keeps invariant at different positions of transceivers. It is determined by the type of LED. Although the position of the transceivers determines the value of $k_{op}(\theta, d)$, the value of $k_{op}(\theta, d)$ is the same at all sub-carriers. It means $k_{op}(\theta, d)$ cannot change neither the shape of SNR nor the shape of the power spectrum of received signal. In other words, we can find that $k_{op}(\theta, d)$ only has an effect on the height of SNR, not the shape. We call it RMIC for generalized VLC channel. Based on the RMIC, the shape of the received signal's power spectrum or SNR depends on the shape of the impulse response of LED.

3. Experimental Study

3.1 Experimental Setup

In order to verify the RMIC, we build a VLC system based on DCO-OFDM for experimental verification.

The experimental setup is illustrated in Fig. 1. Off-line modulation OFDM symbols, from an Arbitrary Waveform Generator (AWG), are superimposed on a proper DC by a bias-T. When we use a cluster of nine white LEDs for experiments, it needs a power amplifier to amplify signal before the bias-T. Then it drives the LED light. At the receiver, we use a commercially available Avalanche Photo Diode (APD) as PD to detect the optical signal, whose detection bandwidth is 100 MHz. A spectrum analyzer is utilized to analyze the power spectrum of the received signal. The details of the experimental setup and instruments are shown in Table 1.

Table 1
The Details of Experimental Setup

Experimental parameters	
FFT size	512
Oversample factor	2
Independent subcarriers number	127
CP length	16/256
Signal bandwidth	50 MHz
AWG sampling rate	200 MHz
Experimental parameters for single LED	
DC	100 mA (3.5 V)
Signal VPP	5 V
Modulation index	0.7
Experimental parameters for a cluster of LEDs	
Number of LEDs	9
DC	350 mA (30 V)
Signal VPP	0.7 V
Amplifier gain	25 dB
Modulation index	0.4
Instrument	
Single LED	Engin, LZ4-04MDCA
A cluster of LEDs	Ouying, 5009
APD	Hamamatsu, C12702-11
Power amplifier	Mini-Circuits, ZHL-6A-S+
Bias-T	Mini-Circuits, ZFBT-6GW-FT+
AWG	Tektronix, AFG3252C
Spectrum Analyzer	Agilent, N9030A

In the experiments, the measured SNR is given by

$$SNR = 10\log_{10}\left(\frac{|X_{sum}|^2 - |N_0|^2}{|N_0|^2}\right), \tag{6}$$

where $|X_{sum}|^2$ is the measured sum power of the received signal and the noise, and $|N_0|^2$ is the measured sum noise power.

3.2 Experimental Result

In the experiment for different incident angles (0 degree, 45 degrees and 60 degrees, respectively) of APD, we measure the received SNR while the distance of transceivers is 0.4 m. The results are illustrated in Fig. 2. Due to the randomness of the noise, the measured SNR fluctuates within a small range, and there is a greater fluctuation when the SNR is low in particular. As the incident angle of APD increases, both the effective area of APD and the measured SNR reduce. At last, the shapes of measured received SNRs are the same at different incident angles of APD.

In the experiment at different distances for a cluster of nine white LEDs, we measure the received SNR at different distance of transceivers (1.6 m, 2.0 m and 2.4 m). The experimental distance setting is based on the practical VLC system. In the practical VLC system, we generally place the receiver on a desk [23]. The height of the desk is 0.85 m in case that the communication distance is about 2.15 m for a typical indoor environment (cubic room, 5 m $\times$ 5 m $\times$ 3 m). Fig. 3 depicts

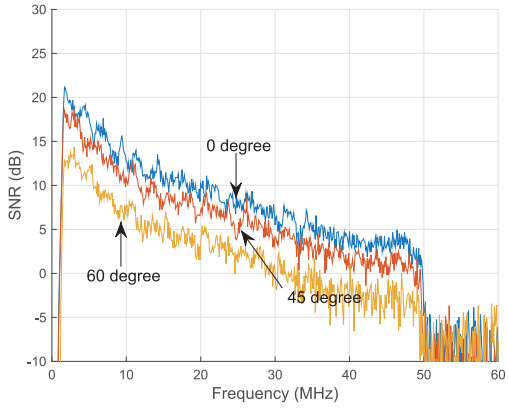

Fig. 2. The received SNR at different incident angles (0 degree, 45 degrees, 60 degrees) of APD.

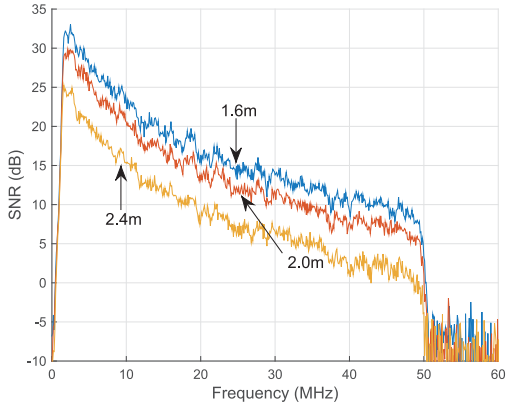

Fig. 3. The received SNR of a cluster of nine white LEDs at different distances (1.6 m, 2.0 m, and 2.4 m).

the results. The shapes of received SNR are nearly the same at different distances and we have verified that the generalized VLC channel has invariant masks of frequency response.

In the experiment for different vertical offsets, we measure the received SNR at different vertical offsets (0 m, 0.3 m and 0.5 m) for a cluster of nine white LEDs. As shown in Fig. 1, we guarantee constant horizontal distance of the transceivers (set to 1.8 m), and move the receiver in the vertical direction. This is close to the practical VLC system, in which the receiver is mobile on the desktop. In this case, while the distance of the transceivers changes, the incident angle of APD also changes. The results are shown in Fig. 4. Under the same horizontal distance, when the vertical offset increases, the distance of the transceivers increases, and the incident angle of APD also increases. According to Lambertian model, the received signal power reduces. Therefore, the received SNR decreases when the vertical offset increases. Moreover, The shapes of received SNRs are unchanged at different vertical offsets. It demonstrates that the generalized VLC channel has the RMIC.

In the experiment at different distances for different colors of LEDs (the white, red, green and blue LED), we measure the received SNR at different distances of transceivers, respectively. Because of the limited power of a single LED, the experimental distances are set to 0.2 m, 0.4 m and 0.75 m. The results are shown in Fig. 5. Due to the bandwidth of transmitted signals is from 0.2 MHz to 50 MHz, the received SNR falls down in frequencies that is higher than 50 MHz. The out-of-band power includes side-lobes leakage power and sum noise power, both of which are very small. Based

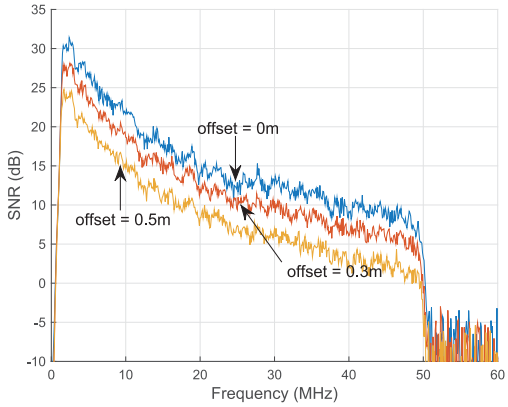

Fig. 4. The received SNR of a cluster of nine white LEDs at different vertical offsets (0 m, 0.3 m and 0.5 m).

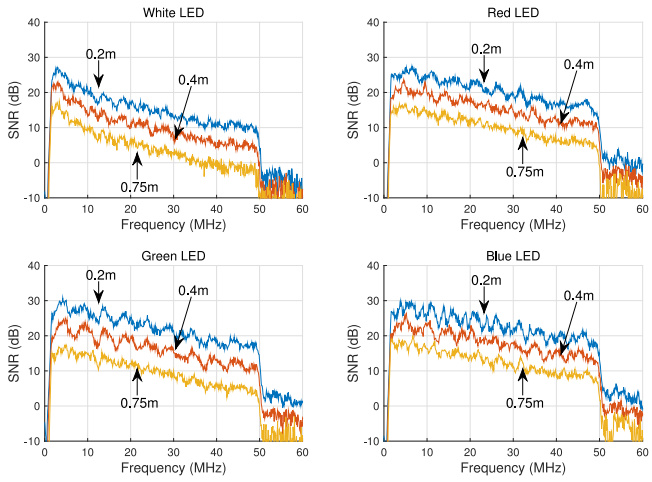

Fig. 5. The received SNR of different colors of LEDs (white, red, green, and blue LED) at different distances (0.2 m, 0.4 m and 0.75 m).

on Lambertian model, the received signal is inversely proportional to the square of the distance. Thus, the received SNR decreases while the distance increases. Besides, there is a jitter for the measured SNR at some frequencies caused by the randomness of the noise. The results also show that different LEDs have different masks of frequency response, which has verified that the shape of the mask depends on the type of LED. The shapes of the received SNR in the same type of LED at different distances approximately are the same. Through the generalized VLC channel, the mask of received SNR has invariant characteristic, which has verified that the RMIC holds with different distances of transceivers.

In summary, the experimental results have verified that the generalize VLC channel has the RMIC.

4. Predefined VLC-OFDM System Design

Based on RMIC, we design a predefined VLC-OFDM baseband with simplified channel feedback. Due to the simplified channel feedback, both the complexity of channel feedback and the data for feedback CSI significantly reduce.

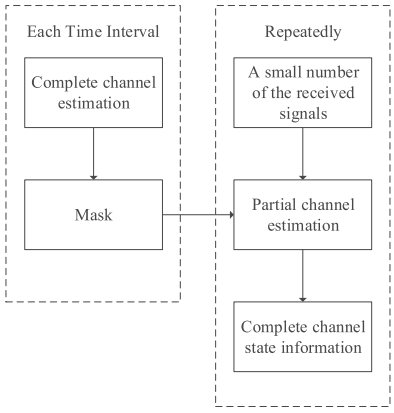

Fig. 6. Flowchart of simplified channel feedback.

4.1 Simplified Channel Feedback

[24]–[26] show that the transmitter cannot finish resource allocation without the feedback CSI or SNR. In VLC system, the feedback link (uplink) need add IR system into existing system while IR need complex design to achieve a high rate [2], [27]. However, the feedback data can significantly reduce based on the feature of RMIC. We propose a new channel feedback method for VLC-OFDM system. In the method, the receiver needn't obtain the distance between transceivers and the incident angle of PD because receiver only sends the relative scaling scalar $\Delta \log(k_{op}^2)$ to the transmitter.

For example, when the first OFDM symbol arrives, the receiver calculates $\log(SNR_k[1])$ denoting the SNR at k-th sub-carrier in the first OFDM symbol. Then the receiver keeps a copy in local memory and sends this mask to the transmitter. When the second OFDM symbol arrives, the receiver also calculates the $\log(SNR_k[2])$. Due to RMIC and Eq. (5), we have

$$\log(SNR_k[2]) - \log(SNR_k[1]) = \log(k_{op}^2[2]) - \log(k_{op}^2[1]) = \Delta \log(k_{op}^2) \tag{7}$$

Note that the OFDM has N sub-carriers, the receiver calculates the mean of $\log(SNR_k[2]) - \log(SNR_k[1])$ to reduce the influence of noise. Then $\Delta \log(k_{op}^2) = \mathrm{E}[\log(SNR_k[2]) - \log(SNR_k[1])]$ is obtained. And so on, when the third OFDM symbol arrives, the new $\Delta \log(k_{op}^2)$ can be given as $\mathrm{E}[\log(SNR_k[3]) - \log(SNR_k[1])]$. Moreover, after a time interval, the receiver will update the mask based on the current OFDM symbol and send a new copy to the transmitter (i.e., update the mask after every one or ten thousand OFDM symbols).

The flowchart of the simplified channel feedback is shown in Fig. 6 and can be concluded as follows:

Step 1. the receiver calculates the mask, keeps a copy in local memory and sends this mask to the transmitter.
Step 2. if it is the time to update mask, then go to Step. 1 else go to Step. 3.
Step 3. When the signal is detected, the receiver calculates the $\Delta \log(k_{op}^2)$ from Eq. (7).
Step 4. The receiver sends the relative scaling scalar $\Delta \log(k_{op}^2)$ to the transmitter through the PD link. Then go to Step. 2.

Due to RMIC, the proposed channel feedback only needs one time slot while the conventional channel feedback needs N time slots in a VLC-OFDM system with N sub-carries.

4.2 Predefined VLC-OFDM Baseband Implement

In this part, we present how RMIC changes the way of designing a VLC system and build a predefined VLC-OFDM system with simplified channel feedback. In addition, the main feature

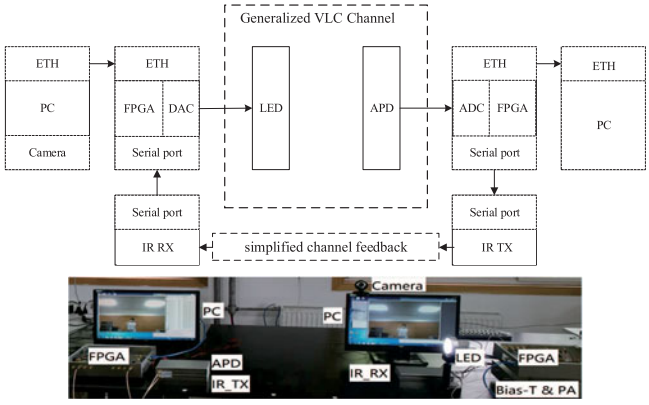

Fig. 7. The structure of the predefined VLC-OFDM system.

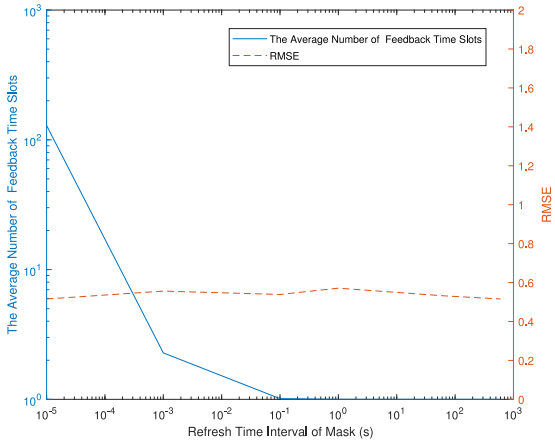

Fig. 8. The performance of the predefined VLC-OFDM system with simplified channel feedback.

of the predefined VLC system is that the transmitter can store the feedback mask of frequency response and use the proposed simplified channel feedback method.

Fig. 7 depicts the predefined VLC-OFDM system. This is a full-duplex wireless optical communication system where downlink is VLC and uplink is IR communication. In our experiment, the predefined VLC-OFDM system with the simplied channel feedback can be used for video transmission and Internet access. In the case of video transmission, the video which is captured by camera is sent from PC to FPGA through Ethernet (ETH).

We change the time interval for the mask feedback, and evaluate the performance through Root Mean Square Error (RMSE) [28]. The RMSE are computed between the received SNR and the SNR measured at the starting time. The performance of the proposed method, simplified channel feedback, is shown in Fig. 8. With the refresh time interval of mask increases, RMSE values keep small and mainly affected by the noise. It can be concluded that the mask of SNR does not change with time. However, the average number of feedback time slots reduces a lot, which means the method can reduce the data for feedback CSI significantly.

Due to the simplified channel feedback, VLC transmitter obtains a complete CSI in an efficient way. The method makes the resource allocation in the transmitter more easier. On one hand, it can reduce the amount of calculations for channel estimation at VLC receiver. On the other hand, the data amount of CSI to be sent in the uplink decreases.

Apart from this, we also verify the BER performance between conventional channel feedback and proposed channel feedback. The VLC system is based on DCO-OFDM with adaptive modulation scheme which is proposed in [29]. In the adaptive modulation scheme, the transmitter calculates

Table 2
The Details of Experimental Setup

Experimental parameters	
FFT size	512
Oversample factor	2
Independent subcarriers number	127
CP length	16/256
Signal bandwidth	50 MHz
AWG sampling rate	200 MHz
The refresh time interval of mask	1 ms

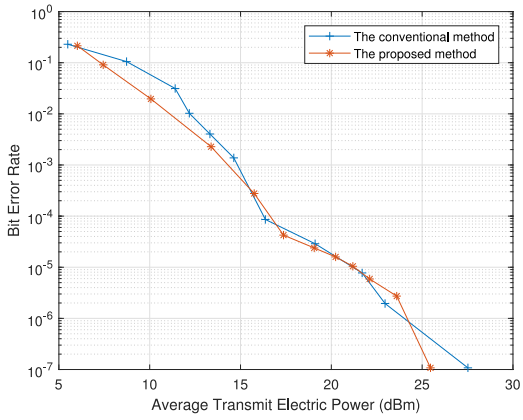

Fig. 9. Comparison of BER performance between proposed method and conventional method.

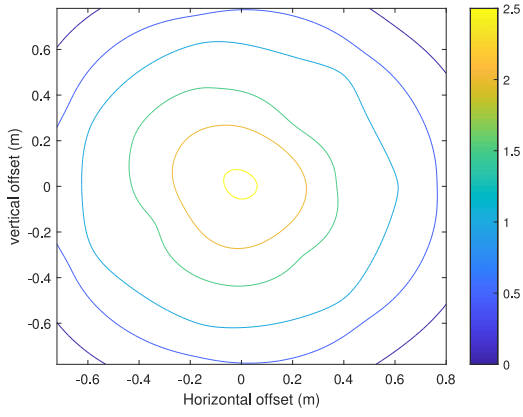

Fig. 10. K_{op} at different positions.

the order of modulation for each sub-carrier based on the mask and the relative scaling scalar. The detailed parameters of OFDM symbol is showed in Table 2.

The comparison of BER performance between proposed method and conventional method is showed as Fig. 9. We can find that there are no significant performance differences between these two methods. It means both two methods can be used for transmitter to obtain a complete CSI/SNR. Moreover, the average number of feedback time slots is 2.3 by using our proposed method while

the conventional channel feedback needs 256 time slots. It can show that our proposed method is in an efficient way.

Besides, we changed the position of receiver and recorded the values of k_{op}. The result is illustrated in Fig. 10. In the figure, the unit of k_{op} is dB, and it shows that k_{op} is determined by the distance between transceivers and the incident angle of PD. The scaling scalar k_{op} decreases while the distance between transceivers and the incident angle of PD increase. Furthermore, the value of k_{op} is almost invariant on the approximate circle because the distances between transceivers and the incident angles of PD are, respectively, the same on these positions.

5. Conclusions

In this paper, we propose the RMIC based on the theoretical analysis of the generalized VLC channel. The RMIC is the main difference between the generalized VLC channel and the RF channel, and it means the shape of frequency response of generalized VLC channel is time-independent and invariant at different positions of the transceivers (including different distances of transceivers, different emitting angles of the LED and different incident angles of the PD). Then we utilize the experimental method to verify the RMIC. Depending on RMIC, we design a new channel estimation feedback method for a predefined VLC-OFDM system where the complexity of channel feedback and the data for feedback CSI significantly reduces.

References

[1] D. Karunatilaka, F. Zafar, V. Kalavally, and R. Parthiban, "Led based indoor visible light communications: State of the art," *IEEE Commun. Surveys Tut.*, vol. 17, no. 3, pp. 1649–1678, Mar. 2015.

[2] K. Lee, H. Park, and J. R. Barry, "Indoor channel characteristics for visible light communications," *IEEE Commun. Lett.*, vol. 15, no. 2, pp. 217–219, Feb. 2011.

[3] S. Long, M. A. Khalighi, M. Wolf, S. Bourennane, and Z. Ghassemlooy, "Investigating channel frequency selectivity in indoor visible-light communication systems," *IET Optoelectron*, vol. 10, no. 3, pp. 80–88, Jun. 2016.

[4] M. Zhang, Y. Zhang, X. Yuan, and J. Zhang, "Mathematic models for a ray tracing method and its applications in wireless optical communications," *Opt. Express*, vol. 18, no. 17, pp. 18 431–18 437, 2010.

[5] H. Elgala, R. Mesleh, and H. Haas, "A study of led nonlinearity effects on optical wireless transmission using OFDM," in *Proc. IEEE IFIP Int. Conf. Wireless Opt. Commun. Netw.*, 2009, pp. 1–5.

[6] H. Elgala, R. Mesleh, and H. Haas, "Non-linearity effects and predistortion in optical ofdm wireless transmission using leds," *Int. J. Ultra Wideband Commun. Syst.*, vol. 1, no. 2, pp. 143–150, 2009.

[7] J. Li, Z. Huang, X. Liu, and Y. Ji, "Hybrid time-frequency domain equalization for led nonlinearity mitigation in OFDM-based VLC systems," *Opt. Express*, vol. 23, no. 1, pp. 611–619, 2015.

[8] I. Stefan, H. Elgala, and H. Haas, "Study of dimming and led nonlinearity for ACO-OFDM based VLC systems," in *Proc. IEEE Wireless Commun. Netw. Conf.*, 2012, pp. 990–994.

[9] L. Chen, W. Wang, and C. Zhang, "Multiuser diversity over parallel and hybrid FSO/RF links and its performance analysis," *IEEE Photon. J.*, vol. 8, no. 3, Jun. 2016, Art. no. 7904909.

[10] L. Chen and W. Wang, "Effective capacity of mimo free-space optical systems over gamma–gamma turbulence channels," *Opt. Commun.*, vol. 382, pp. 450–454, 2017.

[11] L. Chen, W. Wang, and C. Zhang, "Coalition formation for interference management in visible light communication networks," *IEEE Trans. Veh. Technol.*, vol. 66, no. 8, pp. 7278–7285, Aug. 2017.

[12] K. Ying, Z. Yu, R. J. Baxley, H. Qian, G.-K. Chang, and G. T. Zhou, "Nonlinear distortion mitigation in visible light communications," *IEEE Wireless Commun.*, vol. 22, no. 2, pp. 36–45, Apr. 2015.

[13] H. Eliasson, S. L. Olsson, M. Karlsson, and P. A. Andrekson, "Mitigation of nonlinear distortion in hybrid Raman/phase-sensitive amplifier links," *Opt. Express*, vol. 24, no. 2, pp. 888–900, 2016.

[14] D. Tsonev, S. Sinanovic, and H. Haas, "Complete modeling of nonlinear distortion in OFDM-based optical wireless communication," *J. Lightw. Technol.*, vol. 31, no. 18, pp. 3064–3076, 2013.

[15] P. Cruz, N. B. Carvalho, and K. A. Remley, "Evaluation of nonlinear distortion in ADCs using multisines," *Microw. Symp. Dig., 2008 IEEE MTT-S Int.*, pp. 1433–1436, 2008.

[16] J. Armstrong and B. J. Schmidt, "Comparison of asymmetrically clipped optical OFDM and dc-biased optical OFDM in AWGN," *IEEE Commun. Lett.*, vol. 12, no. 5, pp. 343–345, May 2008.

[17] S. D. Dissanayake and J. Armstrong, "Comparison of ACO-OFDM, DCO-OFDM and ADO-OFDM in IM/DD systems," *J. Lightw. Technol.*, vol. 31, no. 7, pp. 1063–1072, 2013.

[18] D. Tsonev, S. Sinanovic, and H. Haas, "Novel unipolar orthogonal frequency division multiplexing (U-OFDM) for optical wireless," in *Proc. IEEE 75th Veh. Technol. Conf, 2012h*, pp. 1–5.

[19] A. Leke and J. M. Cioffi, "A maximum rate loading algorithm for discrete multitone modulation systems," in *Proc. IEEE Global Telecommun. Conf., 1997*, vol. 3, pp. 1514–1518.

[20] O. González, R. Pérez-Jiménez, S. Rodrıguez, J. Rabadán, and A. Ayala, "Adaptive OFDM system for communications over the indoor wireless optical channel," *IEE Proc., Optoelectron.*, vol. 153, no. 4, pp. 139–144, 2006.

[21] H. Elgala, R. Mesleh, and H. Haas, "Indoor optical wireless communication: Potential and state-of-the-art," *IEEE Commun. Mag.*, vol. 49, no. 9, pp. 56–62, Sep. 2011.
[22] C. Nan, *LED Visible Light Communication Technologies*. Beijing, China: Tsinghua Univ. Press, 2013.
[23] T. Komine and M. Nakagawa, "Fundamental analysis for visible-light communication system using led lights," *IEEE Trans. Consum. Electron.*, vol. 50, no. 1, pp. 100–107, Feb. 2004.
[24] W.-C. Kim, C.-S. Bae, S.-Y. Jeon, S.-Y. Pyun, and D.-H. Cho, "Efficient resource allocation for rapid link recovery and visibility in visible-light local area networks," *IEEE Trans. Consum. Electron.*, vol. 56, no. 2, pp. 524–531, May 2010.
[25] D. Tsonev, S. Videv, and H. Haas, "Light fidelity (li-fi): Towards all-optical networking," in *Proc. SPIE*, Vol. 9007, 2014, Art. no. 900702.
[26] M. Kashef, M. Ismail, M. Abdallah, K. A. Qaraqe, and E. Serpedin, "Energy efficient resource allocation for mixed RF/VLC heterogeneous wireless networks," *IEEE J. Select. Areas Commun.*, vol. 34, no. 4, pp. 883–893, Apr. 2016.
[27] V. Tipsuwanporn, P. Chanthosot, V. Krongratana, and A. Numsomran, "Full-duplex star redundant system for visible light communication," in *Proc. World Congr. Eng. Comput. Sci.*, vol. 1, 2017, pp. 256–260.
[28] A. M. Mood, *Introduction to the Theory of Statistics*. New York, NY, USA: McGraw-Hill, 1950.
[29] L. Wu, Z. Zhang, J. Dang, and H. Liu, "Adaptive modulation schemes for visible light communications," *J. Lightw. Technol.*, vol. 33, no. 1, pp. 117–125, 2015.